Hindawi
Journal of Advanced Transportation
Volume 2024, Article ID 6628446, 13 pages
https://doi.org/10.1155/2024/6628446

Research Article

Optimal Reservation Volume of Urban Roads Based on Travel Reservation Strategy

Ruiyu Zhou[1], **Hengrui Chen**[2] and **Hong Chen**[1]

[1]*College of Transportation Engineering, Chang'an University, Xi'an, China*
[2]*School of Transportation, Fujian University of Technology, Fuzhou, China*

Correspondence should be addressed to Hengrui Chen; 2019021060@chd.edu.cn

Received 20 June 2023; Revised 10 December 2023; Accepted 4 January 2024; Published 9 January 2024

Academic Editor: Arkatkar Shriniwas

Improving the spatial-temporal balance between the supply and demand of urban transportation and alleviating traffic congestion are important ways to build sustainable cities. The travel reservation strategy (TRS) is more flexible and refined than traditional traffic demand management methods. This study aims to determine the optimal reservation volume (ORV) for urban roads and verify the effectiveness of the TRS. First, we employed the sustained flow index to estimate the ORV from the degree of trade-off between the road breakdown probability and capacity. Then, a bilevel programming model based on ORV constraints was established to analyse the effectiveness of the TRS. The results indicated that the ORV range is 0.79–0.89 times the road capacity. The TRS can achieve the best steady benefit when the demand for reservation travel reaches at least 40%. Selecting the most congested critical roads in the network to implement TRS is more effective than on a large area. The driver default behavior will increase the V/C ratios and travel costs of all roads in the network. It has been proven that the reservation transportation mode will promote the spatial-temporal balance between supply and demand to alleviate traffic congestion.

1. Introduction

The increasing imbalance between supply and demand in urban transportation systems aggravates traffic congestion. It significantly affects residents' daily lives, causing economic losses and environmental pollution and aggravating the hidden dangers of travel safety [1, 2]. The core cause of traffic congestion is the mismatch between transportation infrastructure supply and residents' travel demand, manifested by the lack of effective traffic demand management measures to adjust to the growing travel demand. With the development of emerging technologies such as instant messaging and artificial intelligence, the travel reservation strategy (TRS) has become a new method for solving urban traffic congestion [3].

TRS is a more flexible and refined traffic supply and demand balance strategy. It refers to the regulation of the total number of vehicles that can pass through the key roads in recurrent congested areas during specific peak hours. The implementation of TRS should first determine the recurrent congested roads and periods that require reservations by monitoring the traffic state of the urban road network. Second, it is crucial to determine the optimal reservation volume (ORV) for the corresponding roads and periods. A small ORV wastes road resources, whereas a large ORV causes road congestion. Therefore, a reasonable ORV is the basis for ensuring the effective implementation of the TRS. Finally, by creating a travel reservation timetable for private cars, travellers can choose the appropriate route and departure time on the reservation platform. Private cars without reservations are prohibited from driving on the reservation road during the reservation period, except buses and special vehicles (such as police cars, fire trucks, and ambulances). TRS can transform queues at roadway bottlenecks into virtual online queues. Travellers can reserve passage roads and time in advance on an open reservation platform, thus realising precise regulation of regional traffic travel demand. Akahane and Kuwahara [4] first introduced a travel reservation method for managing urban traffic demand. They explored the possibility of using reservations to adjust the departure time of travellers to alleviate traffic congestion on holidays. Since then, several studies have applied travel reservations to various scenarios, such as highways [3], urban roads [5], and urban perimeters [6]. The complex network structure and diverse traffic behavior in urban transportation make it more challenging to establish an urban road travel reservation system.

The urban reserved transportation mode is further divided into the regional reservation, road reservation, and lane reservation, according to the scope of the reservation space. A regional reservation strategy means that the traffic demand of an area is limited to below the critical capacity of the area. Only when the area's traffic volume is below the critical capacity can vehicles enter the area. Zhao et al. [6] built a downtown space reservation system to mitigate traffic congestion in a cordon-based downtown area by requiring people who want to drive to this area to make reservations in advance. Menelaou et al. [7] assumed that a heterogeneous urban area is partitioned into multiple homogeneous regions. The vehicle is allowed to enter a region only if it is anticipated that the region will stay within its critical capacity during the time interval that the vehicle will be required to traverse an urban region. The apparent advantage of the regional reservation strategy is that it is easy to implement and only needs to control the boundaries of each region. However, the traffic flow within the region needs to be more delicately managed; otherwise, congestion may still occur, and queuing may occur when entering the region boundary. The lane reservation strategy refers to establishing a high-priority lane on the road for reserved vehicles. Bai et al. [8] showed that the lane reservation strategy could reduce the travel time and air pollution of reserved lanes based on real traffic data. Zhang et al. [9] investigated a bilevel optimisation model for the hazmat transportation problem with lane reservation. They found that the bilevel model can effectively reduce the total risk of hazmat transportation while considering the interests of hazmat carriers and ordinary travellers. The lane reservation strategy will inevitably aggravate traffic congestion in nonreserved lanes; however, the convenience of reserved lanes will gradually change residents' travel concepts. TRS implies that all lanes of a road are only available for reserved vehicles. Menelaou et al. [10] proposed a time-dependent route reservation method for relieving traffic congestion. Some studies have increased the flexibility of travellers' choice of appointment time by introducing evolutionary [11] or pricing [12] mechanisms that combine a dynamic auction with capacity control rules. TRS combines the advantages of road charging and a tradable credit scheme strategy. The core idea of TRS is to encourage travellers to choose a reasonable travel route and period. Through peak load shifting management, travel demands are reasonably arranged in different periods, and congestion queues on the road are transformed into virtual online queues. TRS can alleviate traffic congestion by guiding travel behavior, controlling traffic flow within a reasonable range, and ensuring travel time and speed from departure to destination.

The premise of implementing TRS is to determine ORV. However, previous studies primarily focused on the design of vehicle scheduling models and algorithms for TRS and less on calculating the ORV of reserved roads and analysing the traffic state of the road network under the ORV constraint. Some studies have analysed specific problems with travel reservations by directly setting the reservation volume, such as considering road capacity or the sum of road and parking capacities as the reservation volume [6, 13]. It does not consider the traffic state of reserved roads, which deviates from the essence of TRS. Therefore, in recent years, scholars have preferred to mine traffic flow data to determine reservation volumes [14]. Menelaou et al. [15] replaced the capacity constraint with the density constraint and used infinitesimal perturbation analysis to capture the dynamic change in the critical density value. By comparing the estimated capacity and critical density distribution function, Geistefeldt and Shojaat [16] showed that the relative variability of the capacity is lower than that of the critical density. It revealed that the traffic volume is more appropriate than density to represent the trigger of traffic congestion. Traditionally, road capacity has been treated as a constant value. However, various studies demonstrate that road capacity is not a fixed number but a random variable [17]. Brilon et al. [18] proposed a method to estimate the stochastic capacity function, which can evaluate the breakdown probability for any given volume representing the capacity. Shojaat et al. [19] used the sustained flow index (SFI) to analyse freeway flow performance. The SFI represents the theoretical volume that can maintain fluid traffic under capacity uncertainty. Although stochastic capacity is generally accepted, only a few studies have applied it to quantify road performance in practical traffic management. Furthermore, the complex network structure and various traffic behaviors in urban transportation make it more challenging.

While the literature extensively explores the TRS and its applications, there is a notable dearth of data-driven research specifically targeting its implementation on urban roads. Predominantly, prior studies emphasize vehicle scheduling models and TRS algorithms, sidelining the pivotal task of determining the ORV and assessing the road network's traffic state under ORV constraints. This study seeks to bridge these identified gaps and contribute a novel perspective. To achieve this goal, this study first used the SFI to calculate the ORV of the reservation roads. Then, a bilevel programming model based on ORV constraints was established to explore the influences of the number of reservation roads and reservation tendency on road network capacity, V/C ratio, and travel cost under the implementation of TRS. It can provide managers and decision makers with new ideas for alleviating traffic congestion and determining the critical parameters for implementing TRS.

The rest of this study is organized as follows. Section 2 introduces the method used in this paper in detail. Section 3 conducts a case study with real traffic data and discusses the results. Section 4 concludes this paper.

2. Methodology

2.1. Preliminaries. Setting a scientific and reasonable ORV is the premise of implementing the TRS. It can maximise the reserved road's traffic volume to ensure a smooth road and avoid wasting road resources. Based on the traditional three-phase traffic flow theory (as shown in Figure 1), as the speed increases, the traffic state of the road experiences the evolution process from the "stop-and-go" congested flow to the smooth flow. Therefore, when the road reaches the critical speed, the traffic volume is the theoretical maximum volume. When the road speed exceeds the critical speed, the road remains smooth, but the road resources are not fully utilised. Traffic congestion occurs when the road speed is lower than the critical speed. In the process of traffic flow transition from smooth flow to congestion flow, there is an oscillating region, and traffic flow in this region may lead to congestion once it is subjected to significant external interference. Therefore, determining the critical speed is the key to calculating the optimal total reservation. The speed threshold can be determined by mining the road traffic data. Brilon et al. [18] used the boundary between the upper and lower branches of the speed-flow scatter plot to distinguish noncongested and congested flows. Shojaat et al. [20] determined the speed threshold as the boundary between the fluid and congested traffic by analysing the speed and flow time series. Given this, from the perspective of road network resilience, we used the previous research results to determine the critical threshold of traffic congestion diffusion by using the percolation theory to determine the critical speed of the road [21, 22].

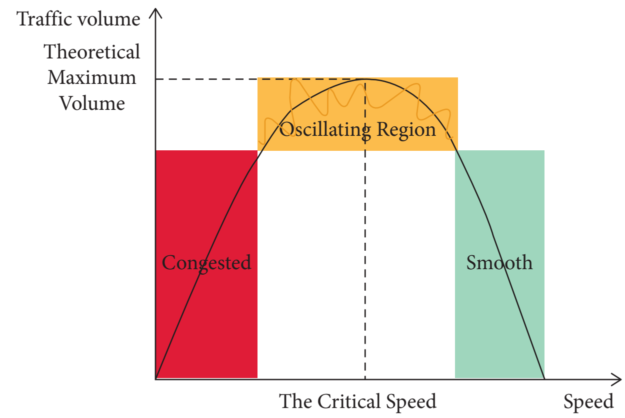

Figure 1: Schematic diagram of theoretical maximum volume.

2.2. ORV Calculation Based on SFI Method. This section describes the ORV calculation method in detail. First, the capacity distribution function of the road is estimated based on the product limit method. The SFI approach is then used to determine the optimal road capacity.

2.2.1. Estimation of the Road Capacity Distribution Function. The capacity distribution function of the road was estimated using the product limit method (PLM) [18]. Capacity is defined as the maximum flow that sustains fluid traffic conditions [23]. The road performance was acceptable when the traffic volume was below the maximum flow. Beyond this flow, the average travel speed drops sharply, causing traffic congestion. The term "breakdown" of the flow has been used to describe the transition from relatively free-flowing traffic to congestion, which is usually called stop-and-go traffic [24]. Generally, the traffic flow observed before the breakdown can be regarded as capacity (momentary). The breakdown can be detected by a sudden and sharp reduction in the traffic speed; therefore, the speed threshold must be determined first. After determining the speed threshold, the period was divided into several time intervals (typically 5 min), and the interval set was defined according to the collected data.

Set B: The average speed in interval i is above the speed threshold and falls below the threshold in the next interval $i+1$, and thus $i \in B$. In this case, the flow in interval i is the traffic volume observed before traffic breakdown, which can be regarded as the momentary capacity of the road.

After determining the set of breakdown intervals, the PLM was used to estimate the road capacity distribution function, and the calculation formula is as follows:

$$F(q) = 1 - S(q) = 1 - \prod_{i:q_i \leq q} \left(\frac{k_i - b_i}{k_i} \right), \quad i \in B, \tag{1}$$

where $F(q)$ is the capacity distribution function, $S(q)$ is the capacity survival function, q is the traffic volume, q_i is the traffic volume in interval i, k_i is the number of intervals with traffic volume $q_i \leq q$, and b_i is the number of breakdowns at volume q_i. B is the set of breakdown intervals.

2.2.2. Determination of ORV Based on SFI Method. The ORV is determined to find an optimal traffic volume in the capacity distribution function to sustain fluid traffic conditions. Shojaat et al. [19] introduced the sustained flow index (SFI) method. The SFI is defined as the product of the traffic volume and probability of survival at that volume, which calculates the theoretical average volume that can be sustained in fluid traffic under capacity uncertainty. The SFI provides a joint performance measure, and the maximum SFI is the best compromise between maximising the volume and minimising the probability of traffic breakdown. Before the maximum SFI, the risk of traffic breakdown was low, but road resources were underutilised. After the maximum SFI is reached, the traffic volume becomes larger and more vulnerable to traffic breakdown. The SFI was calculated using the following formula:

$$\begin{aligned} \mathrm{SFI} &= q_i \cdot S(q_i) \\ &= q_i \cdot (1 - F(q_i)), \end{aligned} \tag{2}$$

where SFI is the sustained flow index, $S(q_i)$ is the probability of survival at volume q_i, and $F(q_i)$ is the probability of breakdown at volume q_i.

The PLM is a nonparametric estimation method that depends on a large number of samples. Obtaining an accurate estimation of the entire capacity distribution function is difficult, and we cannot obtain a relatively accurate maximum SFI. Therefore, it is necessary to know the mathematical distribution functions for parameter estimation. First, we compare the fit of different distributions through experiments and select the most suitable function as the capacity distribution function. Then, we used the SFI to calculate the optimal capacity of the road, as shown in the following equation:

$$\frac{\partial}{\partial q}\left(q\cdot(1-F(q))\right)=1-\left(F(q)+q\cdot f(q)\right)=0, \quad (3)$$

where $f(q)$ is the density function of capacity.

2.3. Bilevel Programming Model Based on ORV Constraints. This study used the weekday morning rush hour as an example to verify the effectiveness of TRS. Travellers who enter reservation roads during this period must make reservations in advance. The traveller must detour if the road has reached the reservation volume. This study assumes that all travellers who have obtained the right-of-way through reservations arrive evenly within the reserved period. The parameters and variables used in this section are listed in Table 1.

The optimal capacity calculated in Section 2.1 is set as the ORV constraint, denoted by q_a^{res}. Therefore, the admissible state of the request of the vehicle j to enter link a in a certain period is denoted by res_a^j. If the request of vehicle j is admissible, $\text{res}_a^j=1$; otherwise, $\text{res}_a^j=0$. Therefore, res_a^j can be calculated as follows:

$$\text{res}_a^j=\begin{cases}1, & \text{if } \sum_{j=1}^{J}\text{res}_a^j\le q_a^{\text{res}}, \quad a\in A_1,\\ 0, & \text{otherwise.}\end{cases} \quad (4)$$

This study divides vehicles into two types: those with reservation tendencies and ordinary vehicles. Vehicles with reservation tendencies will make reservations on the reservation platform before travel and can drive on the reservation road after success. By contrast, ordinary vehicles cannot drive on reservation roads. To simplify the problem, we assume that vehicles with reservation tendencies follow the travel route provided by the reservation system, which is based on the system optimization. In contrast, ordinary vehicle travel is based on the user equilibrium. A bilevel programming (BP) model based on reserved capacity was established to explore the influence of TRS on the traffic state and travel cost of the road network. The upper-level optimisation objective is to maximise the traffic demand, and the constraint condition is the capacity limit of the reservation road. The lower-level optimisation objectives are the system optimal for reservation travellers and user equilibrium for ordinary travellers.

The upper-level model is as follows:

$$\text{Max } Z_{\text{up}}=\sum_{w}\mu^{w}d^{w}, \quad (5)$$

$$\text{s.t. } q_a\le q_a^{\text{res}}, a\in A_1. \quad (6)$$

Table 1: Description of parameters and variables.

Notations	Description
$G=(N,A)$	The transportation network, where N represents the set of nodes and A represents the set of links
a	A directed road link, $a\in A$
A_1	Set of reservation road links, $A_1\subseteq A$
A_2	Set of common road links, $A_2\subseteq A$
W	Set of O-D pairs
w	An O-D pair, $w\in W$
R	Set of paths from origin to destination
r	A path from origin to destination, $r\in R$
q_a	Traffic flow on the link a
q_a^{res}	Optimal reservation volume
res_a^j	The admissible state of the request of the vehicle j to enter the link a
μ^w	O-D pair w demand multiplier
d^w	The original travel demand for O-D pair w
λ	The reservation tendency
u_r^w	The traffic flow on the path r on the OD pair w
$\delta_{a,r}^w$	The path-link relation: if the link a is on the path r between O-D pair w, then $\delta_{a,r}^w=1$; otherwise, $\delta_{a,r}^w=0$
ε_r^w	The reservation section-path relation: if there is no reservation section on the path r between O-D pair w, then $\varepsilon_r^w=1$; otherwise, $\varepsilon_r^w=0$
$t_a(q_a)$	The travel cost function of link a
t_a^0	The free flow time of link a
C_a	The capacity of the link a

Equation (5) shows the objective function of the upper-level model. w is a set of OD pairs and $w\in W$; d^w represents the original travel demand for the OD pair w. μ^w is the OD pair w and the value of μ indicates whether the current network capacity has spare capacity [25]. If $\mu>1$, the network has a spare capacity; otherwise, the network is overloaded. $\sum_w\mu^w d^w$ represents the total capacity of the road network. Equation (6) represents the capacity constraint on the reservation road, where q_a is the traffic flow on link a.

Under the TRS, two types of travellers exist in the road network that pursue optimisation under the influence of each other. The lower-level model is a mixed traffic equilibrium model, which can be expressed as follows:

$$\text{Min } Z_{\text{down}}^{\text{so}}=\sum_{a}q_a^{\text{so}}\times t_a\left(q_a^{\text{so}}+q_a^{\text{ue}}\right), \quad (7)$$

$$\text{s.t. } d_w^{\text{so}}=\lambda\mu^{w}d^{w}, \quad \forall w\in W, \quad (8)$$

$$d_w^{\text{so}}=\sum_{r}u_r^{\text{so},w}, \quad \forall w\in W, r\in R, \quad (9)$$

$$q_a^{\text{so}}=\sum_{w}\sum_{r}u_r^{\text{so},w}\delta_{a,r}^{\text{so},w}, \quad \forall w\in W, r\in R, a\in A, \quad (10)$$

$$q_a^{\text{so}}\ge 0, u_r^{\text{so},w}\ge 0, \quad \forall w\in W, r\in R, a\in A. \quad (11)$$

Equation (7) is the objective function of the system optimal model, which is constrained by equations (8)–(11). q_a^{so} and q_a^{ue} represent traffic flow on link a under the system optimal and user equilibrium model, respectively. $t_a(q)$ is the travel cost function of link a. Equation (8) represents the flow conservation constraints scaled by the OD matrix multiplier μ. μ is a variable from the upper-level program. d_w^{so} represents the travel demand of the reservation-tendency vehicle and λ is the reservation tendency. Equation (9) ensures that the sum of the flows assigned to paths equals the travel demand, where R represents the set of paths, $r \in R$, and $u_r^{\mathrm{so},w}$ is the traffic flow on path r on the OD pair w. Equation (10) ensures that the sum of all path flows through link a is equal to q_a^{so}. $\delta_{a,r}^{\mathrm{so},w}$ are path-link relations. If link a is on path r, then $\delta_{a,r}^{\mathrm{so},w} = 1$; otherwise, $\delta_{a,r}^{\mathrm{so},w} = 0$. Equation (11) indicates that the variables are positive.

$$\mathrm{Min}\ Z_{\mathrm{down}}^{\mathrm{ue}} = \sum_a \int_0^{q_a^{\mathrm{ue}}} t_a\left(q_a^{so} + q\right)\mathrm{d}q, \tag{12}$$

$$\text{s.t. } d_w^{\mathrm{ue}} = (1-\lambda)\mu^w d^w, \quad \forall w \in W, \tag{13}$$

$$d_w^{\mathrm{ue}} = \sum_w u_r^{\mathrm{ue},w}\varepsilon_r^{\mathrm{ue},w}, \quad \forall w \in W, r \in R, \tag{14}$$

$$q_a^{\mathrm{ue}} = \sum_w \sum_r u_r^{\mathrm{ue},w}\delta_{a,r}^{\mathrm{ue},w}, \quad \forall w \in W, r \in R, a \in A_2, \tag{15}$$

$$q_a \geq 0, u_r^{\mathrm{ue},w} \geq 0, \quad \forall w \in W, r \in R, a \in A_2. \tag{16}$$

Equation (12) represents the objective function of the user equilibrium model, which is constrained by equations (13)–(16). In equation (13), d_w^{ue} represents the travel demand of an ordinary vehicle. Equation (14) ensures that the sum of the flows assigned to paths equals the travel demand, where $u_r^{\mathrm{ue},w}$ is the traffic flow on the path r on the OD pair w. $\varepsilon_r^{\mathrm{ue},w}$ is the reservation section-path relation, which ensures that ordinary vehicles cannot enter the exclusive section of the reservation travel. If no reservation section exists on path r, then $\varepsilon_r^{\mathrm{ue},w} = 1$; otherwise, $\varepsilon_r^{\mathrm{ue},w} = 0$. Equation (15) ensures that the sum of all path flows through link a is equal to q_a^{ue}. $\delta_{a,r}^{\mathrm{ue},w}$ are path-link relations. If link a is on path r, then $\delta_{a,r}^{\mathrm{ue},w} = 1$; otherwise, $\delta_{a,r}^{\mathrm{ue},w} = 0$. Equation (16) indicates that the variables are positive.

This study used the BPR function as the performance function:

$$t_a\left(q_a\right) = t_a^0\left[1 + \alpha\left(\frac{q_a}{C_a}\right)^{\beta}\right], \tag{17}$$

where α and β are fixed parameters, which are assumed to be $\alpha = 2.05$ and $\beta = 4$. We used the least squares method combined with GPS and historical traffic data to determine the values of α and β by fitting the function. We used calibration values to ensure that the BPR function accurately represents the observed relationship between travel time and traffic flow in the study area. Given the limited length of this study and the fact that the parameter calibration process has been widely used in previous studies [26–28], we will not elaborate on it again in this paper.

The solution efficiency was significantly reduced because of the numerous roads in the study area while solving the BP model. Surrogate models (e.g., polynomial regression, radial basis function, neural networks, and Kriging models) have been applied to transportation problems in recent years because of their superior computational speed and good analytical properties [29, 30]. Some studies have indicated that the Kriging model has the highest fitting accuracy [31]. Therefore, this study adopted the Kriging model to solve the BP model. A single-projection algorithm was used to solve the lower-level model. Refer to [32–34] for more details. The specific modelling and solving steps of the Kriging model are as follows [35, 36].

The Kriging model is an interpolation method, and its interpolation result is defined as the linear weighting of the response value of all sample points.

$$\hat{y}(x) = \sum_{i=1}^{n} \varpi^{(i)} y^{(i)}. \tag{18}$$

As long as the weighting coefficient ϖ is provided, the performance prediction value of any scheme in the design space can be obtained. To calculate the weighting coefficients, the unknown function was regarded as a Gaussian process.

$$Y(x) = \beta_0 + Z(x), \tag{19}$$

where β_0 is an unknown constant and the mathematical expectation of $Y(x)$ and $Z(x)$ is a stochastic process with a mean of 0 and a variance of σ^2. In the design space, these random variables are correlated and their covariance is

$$\mathrm{Cov}\left[Z(x), Z'(x)\right] = \sigma^2 R\left(x, x'\right), \tag{20}$$

where $R(x, x')$ is the correlation function. This study adopts the Gaussian exponential model:

$$R\left(x, x'\right) = \exp\left(-\theta \sum_{k=1}^{n} \left\|x - x'\right\|^2\right), \tag{21}$$

where θ is the hyperparameter. The maximum likelihood estimation was used for hyperparameter training to increase the solving accuracy of the model. Because the values of hyperparameters cannot be provided analytically, hyperparameter training is generally solved using numerical optimisation methods such as genetic, simulated annealing, and nongradient algorithms. In this study, a simulated annealing algorithm was used.

Based on the above assumptions, the Kriging model aims to find the optimal weighting coefficient ϖ so that the following mean square error is minimised and unbiased condition is satisfied.

$$\mathrm{MSE}\left[\hat{y}(x)\right] = E\left[\left(\boldsymbol{\varpi}^{\mathrm{T}}\mathbf{Y}_{\mathbf{s}} - Y(x)\right)^2\right]. \tag{22}$$

Using the Lagrange multiplier method, the Kriging model can be obtained through derivation:

$$\begin{aligned}
\hat{y}(x) &= \begin{bmatrix} \mathbf{r}(\mathbf{x}) \\ 1 \end{bmatrix}^T \begin{bmatrix} \mathbf{R} & \mathbf{F} \\ \mathbf{F}^{\mathbf{T}} & 0 \end{bmatrix}^{-1} \begin{bmatrix} y_s \\ 0 \end{bmatrix}, \\
\mathbf{F} &= \begin{bmatrix} 1 & 1 & \cdots & 1 \end{bmatrix}^T, \\
\mathbf{r}(\mathbf{x}) &= \begin{bmatrix} R\left(x^{(1)}, x\right) \\ \vdots \\ R\left(x^{(n)}, x\right) \end{bmatrix}, \\
\mathbf{R} &= \begin{bmatrix} R\left(x^{(1)}, x^{(1)}\right) & \cdots & R\left(x^{(1)}, x^{(n)}\right) \\ \vdots & \cdots & \vdots \\ R\left(x^{(n)}, x^{(1)}\right) & \cdots & R\left(x^{(n)}, x^{(n)}\right) \end{bmatrix}.
\end{aligned} \tag{23}$$

The Kriging model is an interpolation model, and the infill criterion generally adopts expected improvement (EI) maximisation to generate new sample points. Let the current optimal objective function value be y_{best} and let the Kriging prediction result satisfy the normal distribution with mean $\hat{y}(x)$ and standard deviation $s(x)$.

The expected improvement at point x is expressed as follows:

$$E[I(x)] = \begin{cases} \left(y_{\text{best}} - \hat{y}\right)\Phi\left(\dfrac{y_{\text{best}} - \hat{y}}{s}\right) + s\phi\left(\dfrac{y_{\text{best}} - \hat{y}}{s}\right), & s > 0, \\ 0, & s = 0, \end{cases} \tag{24}$$

where $I(x)$ is the improvement at point x and Φ and ϕ are functions of the standard normal cumulative distribution and standard normal distribution probability density, respectively. The new sample point can be obtained by solving the suboptimization problem that maximizes the $E[I(x)]$.

Because the road capacity constraint is a strong constraint, this study adopts the penalty method to incorporate it into the objective function while solving the BP model, and the objective function is as follows:

$$\max z_0 = \sum_w d^w + \tau\left(q_a^{\text{res}} - q_a\right), \quad a \in A_1, \tag{25}$$

where τ is the penalty coefficient. The specific solution algorithm is given below:

Step 1. Enter the maximum number of iterations $N_{\max}$, maximum consecutive successes $C_{\text{succ}}^{\max}$, maximum consecutive failures $C_{\text{fail}}^{\max}$, and the initial perturbation probability p_{select}^0. Generate an initial set of evaluation points I_0 using Latin hypercube sampling and set the number of iterations $n = 0$.

Step 2. Obtain the vector of objective function values for all evaluation points $\mathbf{Z} = [Z(Q_i), Q_i \in I_0]$ and the current optimal solution Q_{best}.

Step 3. Based on the evaluation point set I_n, the simulated annealing method is used to obtain the hyperparameters and update the Kriging model.

Step 4. Based on the current optimal solution $\mathbf{y}_{\text{best}}$ and perturbation probability p_{select}^n, the simulated annealing method is used to solve the maximum EI to obtain the candidate point $\mathbf{y}_{n+1}$.

Step 5. The single-projection algorithm is used to solve the lower-level mixed traffic equilibrium model and then calculate $Z(y_{n+1})$.

Step 6. If $Z(y_{n+1}) < Z(y_{\text{best}})$, then $y_{\text{best}} = y_{n+1}$, $Z(y_{\text{best}}) = Z(y_{n+1})$, continuous success count $C_{\text{succ}} = C_{\text{succ}} + 1$, and consecutive failure count $C_{\text{fail}} = 0$; otherwise, $C_{\text{fail}} = C_{\text{fail}} + 1$ and $C_{\text{succ}} = 0$.

Step 7. Update the set of evaluation points $I_{n+1} = I_n \cup \{y_{n+1}\}$. If $C_{\text{succ}} > C_{\text{succ}}^{\max}$, then $p_{\text{select}}^{n+1} = p_{\text{select}}^n/2$ and $C_{\text{succ}} = 0$. If $C_{\text{fail}} > C_{\text{fail}}^{\max}$, then $p_{\text{select}}^{n+1} = 2 * p_{\text{select}}^n$ and $C_{\text{fail}} = 0$. Set $n = n + 1$.

Step 8. If $n \geq N_{\max}$, stop, and output y_{best}. Otherwise, return to Step 3.

3. Experiments and Analysis

This section presents a case study that demonstrates the effectiveness of the proposed methodology. This could provide essential parameter values for implementing the TRS in a specific environment, which provides a theoretical and practical basis for the promotion of the strategy.

3.1. Study Area and Data Description. As the most important political and cultural centre in Northwest China, Xi'an is the beginning of the ancient Silk Road and an important node of the "One Belt, One Road" policy. Therefore, improving the intellectual level of urban traffic management and relieving urban traffic congestion are urgent. This study took part of the urban road network in Xi'an, China, as the study area, including 19 nodes and 56 directional links, as shown in Figure 1 The label on the link in Figure 2 is denoted by (t_a^0, C_a). Links 3-8-11-16 and 16-11-8-3 are commuter roads with large traffic flow and obvious congestion during peak hours. Therefore, we chose these links as reservation roads, and the reservation period was from 8:00 to 9:00 in the morning rush hour. During this period, only reserved vehicles could enter the reserved roads.

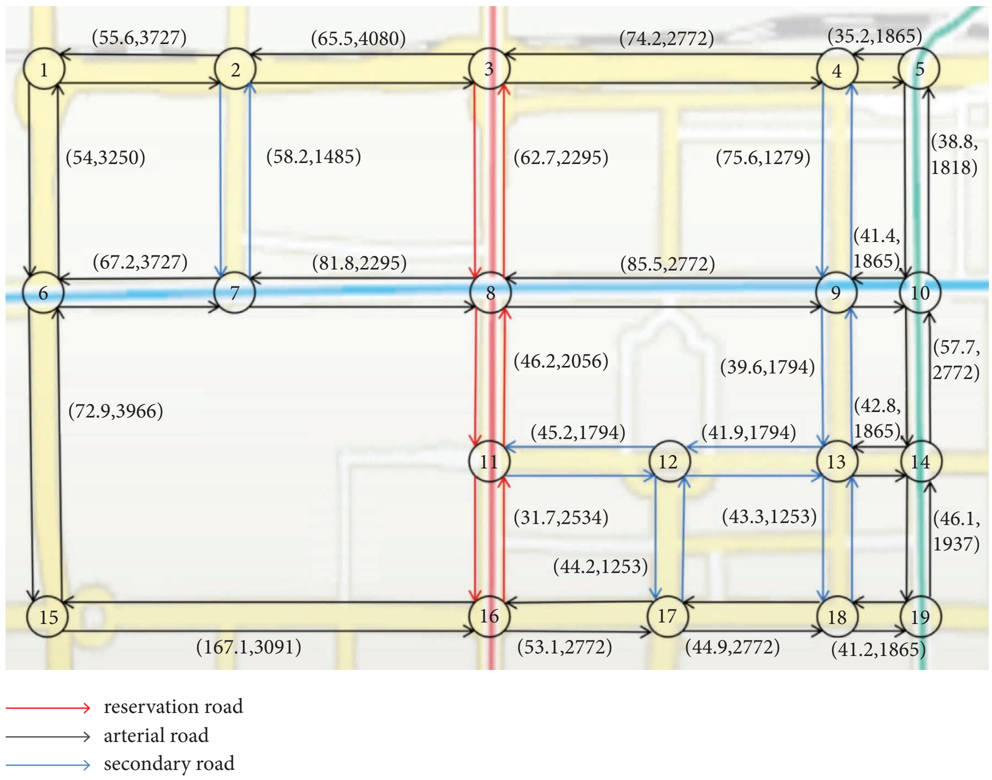

Figure 2: The study area.

This study used the geomagnetic sensor data during the working days in Xi'an, China, in June 2019, and obtained the initial traffic demand (as shown in Table 2) by OD matrix inversion.

Parameter values of the BP algorithm are as follows: maximum number of iterations $N_{\max} = 200$, maximum consecutive successes $C_{\text{succ}}^{\max} = 3$, maximum consecutive failures $C_{\text{fail}}^{\max} = 3$, and initial perturbation probability $p_{\text{select}}^{0} = 0.5$. Parameter values of the single-projection algorithm of the lower-level model are as follows: the projection step size was 0.01, convergence accuracy was 1×10^{-5}, and path set update frequency was 20.

Table 2: Initial traffic demand (vph).

Origin	Destination					
	1	3	5	15	16	19
1	0	916	1104	1007	2809	263
3	282	0	1004	916	1307	1187
5	597	1210	0	651	151	1304
15	396	400	136	0	2795	1745
16	3624	640	248	2050	0	436
19	246	1137	993	1596	1503	0

3.2. Calculation of Reservation Road ORV. As mentioned before, from the perspective of road network resilience, we used the previous research results to determine the critical threshold of traffic congestion diffusion by using the percolation theory to determine the critical speed of the road [21, 22]. The critical speed of reserved road was approximately 30 km/h. Referring to the research on the road capacity distribution function in highway scenarios [19], this study first used the PLM to estimate the road capacity distribution function ($F(q)$) according to equation (1). The PLM is a nonparametric estimation method that cannot estimate the complete $F(q)$. Therefore, three types of functions with analytical solutions (Weibull, logistic, and Gumbel distributions) were used in this study to fit the distribution function of road capacity. Finally, the best-fitting function was selected, and the optimal volume was determined by estimating the corresponding SFI based on equation (3). The calculation results are presented in Figure 3 and Table 3.

As shown in Table 3, the logistic distribution function has the largest adjusted R-squared value and the smallest residual sum of squares compared to the other two distribution functions. Moreover, combined with Figure 3, the logistic distribution function was more consistent with the evolution law of the road capacity distribution function. The calibration parameters γ and ϑ under the logistic distribution were 2292.323 and 188.513, respectively. By substituting the parameters into Table 3, the optimal volume of the logistic distribution and the corresponding breakdown probability were calculated to be 1879 vph and 0.1, respectively, as shown at point B in Figure 3. When the flow rate was 1879 vph, SFI reached a maximum value of 1691 vph. The link performance reaches its maximum value, as shown at point A in Figure 3. The breakdown probability increased when the flow rate was greater than 1879 vph, which increased the probability of congestion. Although the

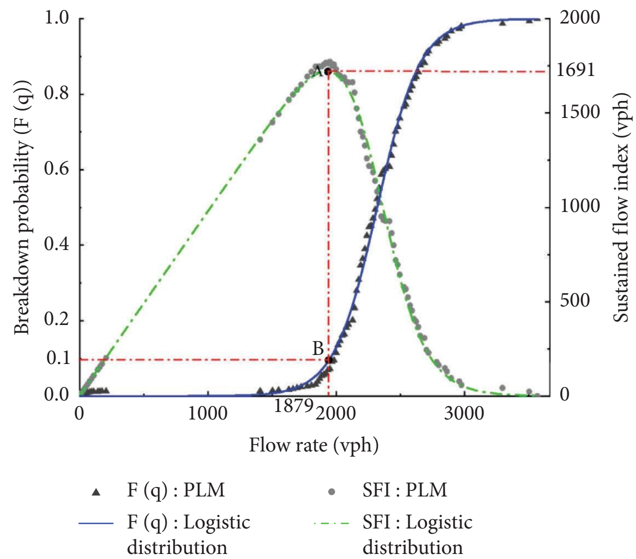

Figure 3: Capacity distribution function and sustained flow index of the link 8-11.

Table 3: Goodness of fit for different distribution functions.

Distribution type	$F(q)$	Optimal volume (vph)	Adjusted R-squared	Residual sum of squares
Weibull	$1 - e^{-(q/\vartheta)^{\gamma}}$	$\vartheta(1/\gamma)^{1/\gamma}$	0.983	0.070
Logistic	$1/1 + e^{-q-\gamma/\vartheta}$	$\vartheta(W(e^{\gamma/\vartheta-1}) + 1)$	0.988	0.024
Gumbel	$1 - e^{-e^{q-\gamma/\vartheta}}$	$\vartheta(W(e^{\gamma/\vartheta}))$	0.970	0.111

Note. W = Lambert function; γ = shape; ϑ = scale.

breakdown probability is reduced when the flow rate is less than 1879 vph, the low flow rate indicates that road resources are not completely utilised. In summary, the ORV for link 8-11 was 1879 vph.

The same method was used to determine the best-fit function and optimal road volume. Table 4 shows the results for the different links. As shown in Table 4, the Weibull and logistic distribution functions provided the best fitting effect for urban roads. The adjusted R-squares were all above 0.95, and the residual sum of squares was below 0.2. Considering the highways, most roads were suitable for the Weibull distribution. Table 4 also shows the best-fit distribution, calibrated parameters, optimal volumes, and breakdown probabilities of different links. The results indicated that the optimal volume range is 0.79–0.89 times the road capacity. Previous studies have demonstrated that the breakdown probability of highways is approximately 5% [19]. The breakdown probability of urban roads mostly exceeded 10%, indicating that urban roads face a greater risk of traffic congestion than highways. This is primarily owing to the complex road conditions of urban roads, such as signal lights, poor driving habits, and the influence of pedestrians and nonmotor vehicles [37].

This study assumed that the traffic demand of the road network remained unchanged before and after the implementation of TRS. The rationality of ORV is verified by comparing the original traffic assignment (no reservation roads in the network) results based on user equilibrium and the results after implementing TRS. As mentioned above, links 3-8-11-16 and 16-11-8-3 are set as reservation links during the morning rush hour. Therefore, only reserved vehicles can drive into these links during this period. The ORV and road capacity constraints (C_a) of each link are substituted into the BP model, and the calculation results are listed in Table 5.

As shown in Table 5, the average V/C ratio of the arterial road is 0.931 before strategy implementation, indicating severe traffic congestion. However, the average V/C ratio of the secondary road was only 0.278, indicating that road resources were not completely utilised. After the strategy implementation, the congestion of the arterial road is alleviated, the usage of secondary road resources increases, and the total travel cost is reduced. It has been proven that implementing this strategy reduces traffic congestion on the road network and alleviates the imbalance of traffic flow in spatial distribution. Further observation shows that under the ORV constraint, the travel cost is lower and the V/C ratio of the arterial road is lower, which proves that it is reasonable to determine the road reservation capacity using the SFI method.

3.3. Verification of TRS Effectiveness. This section explores the effect of different factors (e.g., reservation tendency and number of reservation roads) on the road network capacity, service level, and travel cost, as shown in Figures 4(a)–4(c)).

Figure 4(a) shows the calculation results of the road network capacity under different numbers of reservation roads and λ. The dotted line indicates the network capacity

Table 4: Different link results.

Link	Adjusted R-squared			Residual sum of squares			The results under the best-fitting distribution				
	Weibull	Logistic	Gumbel	Weibull	Logistic	Gumbel	γ	ϑ	Optimal volume (vph)	Optimal volume/C_a	Breakdown probability (%)
3-8	0.952	0.909	0.867	0.088	0.166	0.244	6.558	2721.177	2043	0.89	0.141
8-3	0.967	0.933	0.889	0.055	0.113	0.186	6.883	2425.898	1833	0.80	0.135
11-8	0.983	0.981	0.979	0.021	0.024	0.140	7.974	2300.002	1773	0.86	0.118
11-16	0.981	0.982	0.963	0.186	0.177	0.593	2398.322	179.836	1984	0.78	0.091
16-11	0.988	0.989	0.981	0.018	0.017	0.139	2511.187	184.919	2081	0.82	0.089
6-7	0.980	0.974	0.971	0.021	0.033	0.249	6.888	4221.177	3190	0.85	0.135
7-6	0.978	0.979	0.969	0.023	0.021	0.140	3492.563	261.874	2889	0.78	0.091
7-8	0.988	0.988	0.972	0.007	0.010	0.156	8.493	2508.955	1950	0.85	0.111
8-7	0.983	0.978	0.958	0.015	0.024	0.348	7.848	2386.806	1836	0.80	0.120
8-9	0.984	0.986	0.964	0.019	0.013	0.247	2762.480	237.576	2254	0.81	0.105
9-8	0.987	0.982	0.975	0.009	0.022	0.184	8.493	2908.955	2261	0.82	0.111
9-10	0.984	0.982	0.961	0.013	0.018	0.246	9.546	1853.874	1464	0.78	0.099
10-9	0.979	0.978	0.968	0.020	0.041	0.258	9.179	2053.658	1613	0.86	0.103

Table 5: V/C ratio and travel costs after implementing the TRS.

		Average V/C of all links	Average V/C of arterial links	Average V/C of secondary links	Average V/C of reservation links	Travel costs of all links (s)
Before ORV	Original traffic assignment	0.849	0.931	0.278	0.946	10636952
After ORV	ORC constraints	0.791	0.821	0.585	0.661	8655867
	C_a constraints	0.827	0.874	0.501	0.640	9555154

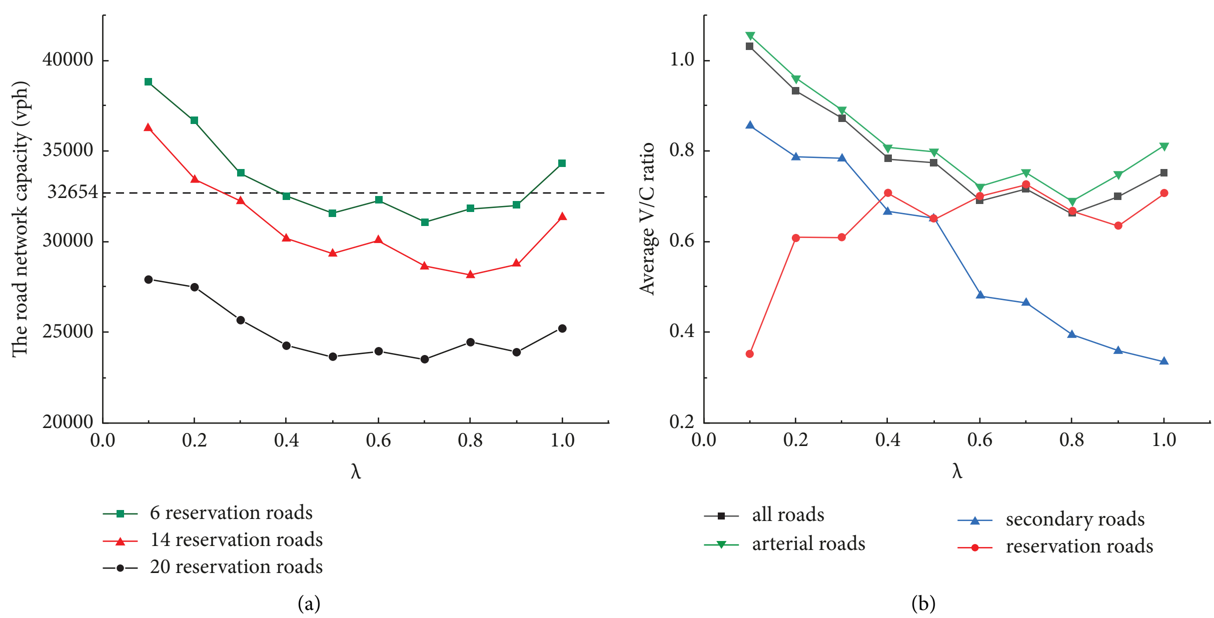

Figure 4: Continued.

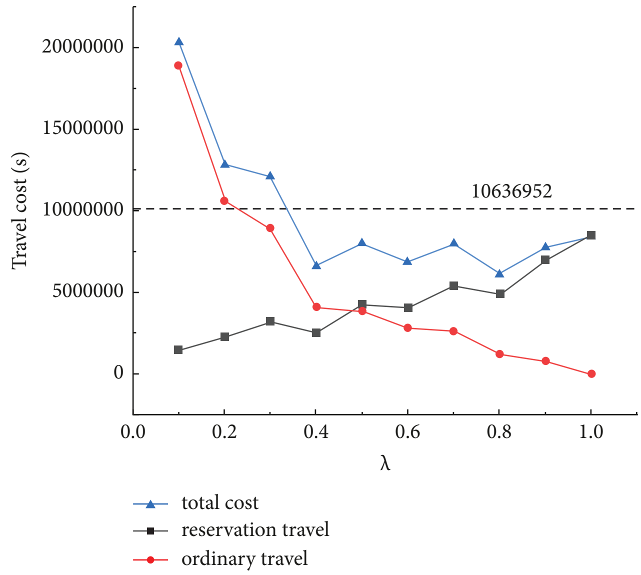

(c)

Figure 4: Sensitivity analysis. (a) Road network capacity under different scenarios. (b) Average V/C ratios under different conditions. (c) Travel costs for different situations.

in the original traffic assignment. It can be observed that under the same conditions, the larger the number of reservation roads, the smaller the road network capacity. Setting reservation roads is equivalent to adding capacity restrictions to these roads. Although it can improve the congestion of reservation roads to a certain extent, it also increases the traffic pressure on surrounding roads and causes the congestion to spread to other roads. Given this, it is unreasonable to set up numerous reservation roads during peak hours. Therefore, selecting the most congested critical roads in the network is necessary to implement the TRS. With the same number of reservation roads, the network capacity decreases and finally becomes stable with the increase in λ. The network capacity is stable at a value less than the original capacity, indicating that the network traffic surges in the morning peak hour, the road network is congested, and there is no spare capacity in the network. Some travellers need to adjust their departure time. When λ reaches 0.4, the network capacity reaches a stable state. Combined with Figures 4(b) and 4(c), it can be found that when λ reaches 0.4, the V/C ratio and travel cost of the network both reach a stable state. Therefore, the TRS achieves the best benefit when the demand for reservation travel reaches at least 40%. This stable network capacity is the optimal capacity for travel during peak hours under the reservation policy. The road network capacity is controlled within this range to achieve peak load shifting management of traffic flow so that the queuing of vehicles on the road during the extreme congestion period becomes the queuing of online reservations, thereby reducing road traffic congestion. Therefore, adopting the TRS for critical roads with extreme congestion is a dynamic constraint that can realise the dynamic adjustment of travel demand.

We further discuss the service level change of different grade roads in the network with different λ values under the six reservation roads, and the results are shown in Figure 4(b). With an increase in λ, the different grades of roads indicated different evolution trends. The average V/C ratios of all roads, arterial roads, and secondary roads decreased gradually with an increase in λ. When the value of λ is small, the reservation travel demand is low, and the resources of the reservation roads are not effectively utilised, resulting in the remaining roads bearing part of the traffic volume of the reservation roads with a large V/C ratio of the remaining roads. With an increase in λ, the V/C ratio of the reservation roads first increased and finally stabilised. After $\lambda = 0.4$, the average V/C ratios of all roads and reservation roads are stable at approximately 0.726 and 0.685, respectively. Because the ORV is set on the reservation roads, the traffic flow exceeding the ORV cannot enter the reservation roads; therefore, the V/C ratio of the reservation road will remain stable and acceptable. In conclusion, combined with the results in Table 5, it can be found that the TRS can alleviate the time-space mismatch between supply and demand to a certain extent and reduce queuing on the road under limited resource conditions.

Figure 4(c) shows the travel cost change of different modes in the network with different λ values under the six reservation roads. With an increase in λ, the travel cost of the ordinary mode first decreased and finally stabilised, while the travel cost of the reservation mode first increased and then stabilised. Initially, drivers who adopt the reservation mode can enjoy smooth travel. However, with an increase in reservation users, the traffic flow of the reservation road gradually increases, which leads to an increase in the V/C ratio and travel costs. After $\lambda = 0.4$, owing to the ORC

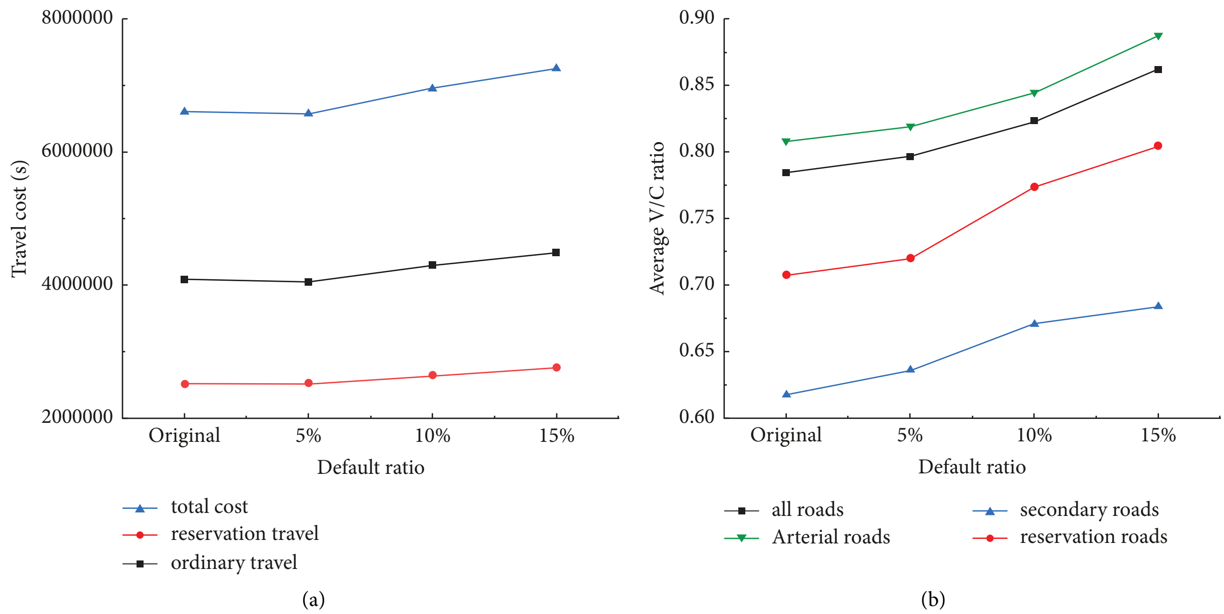

Figure 5: The effects of varying degrees of driver compliance on the results. (a) Travel costs under different default ratios. (b) Average V/C ratios under different default ratios.

limitation, some users cannot make a reservation and choose to take a detour; therefore, the travel cost of the reservation mode is stable. In addition, with an increase in λ, the total travel cost of the road network first decreased and finally stabilised. It shows that implementing TRS can alleviate urban traffic congestion to a certain extent and reduce travel costs for residents.

Moreover, we explored the effects of varying degrees of driver compliance on the results. Specifically, we set six reservation roads and $\lambda = 0.4$ and evaluated the impact on road network service level and travel cost by considering cases where a certain percentage of drivers did not comply with the proposed policy. The default ratio of 5% means that 5% of travellers who have not obtained the right-of-way violate the regulations and pass through the reserved roads. As shown in Figure 5(a), the travel cost in both reservation and ordinary modes gradually increases with the increase of the default ratio. It can be understood as defaulting by some travellers leading to the reservation road's traffic volume exceeding the ORV, exacerbating congestion and delays on the reservation roads, and affecting other travellers' itineraries. As depicted in Figure 5(b), the driver's default behavior can have an adverse effect on the V/C ratios of the entire road network. The roads in the road network are interconnected. Therefore, when the congestion on the reservation roads increases sharply, it affects the surrounding roads. These roads are also affected, with reduced travel speed, vehicle queues, and more severe congestion. In summary, the driver default behavior can lead to traffic congestion and increase the V/C ratios and travel costs of all roads in the network. Therefore, we must adopt appropriate reward and punishment measures and improve the supporting monitoring system to encourage drivers to abide by the rules and avoid default behaviors.

4. Conclusion

This study aimed to determine the optimal reservation volume (ORV) of urban roads and verify the effectiveness of the travel reservation strategy (TRS). We employed the sustained flow index (SFI) to estimate the ORV from the degree of trade-off between road breakdown probability and capacity. A bilevel programming model based on ORV constraints was established to explore the influences of the number of reservation roads and reservation tendency on road network capacity, V/C ratio, and travel cost under the implementation of TRS. The effectiveness of this strategy was verified by mining the road traffic characteristics using geomagnetic sensor data. The contributions of this study are summarised as follows: (1) it is one of the few data-driven attempts to discuss the implementation of TRS on urban roads; (2) the proposed ORV can be widely used in general studies of urban road network scenarios, such as optimisation of traffic control strategies and vehicle routing during emergencies; (3) it verifies the effectiveness of TRS on urban roads, which helps alleviate the spatial-temporal mismatch between the supply and demand, reducing queuing on the road under limited resource conditions and helping promote sustainable city construction; and (4) crucially, the research elucidates that during peak hours, TRS should target key congested road segments and becomes most effective when at least 40% of vehicles are reserved, providing actionable insights for urban traffic policymakers.

The case analysis results indicate that (1) the Weibull distribution is more consistent with the evolution tendency of the road capacity distribution function, and the ORV range is 0.79–0.89 times the road capacity; (2) it is more effective to select the most congested critical roads in the network to implement TRS than a large area; (3) the TRS can achieve best steady benefit when the demand for reservation travel reaches at least 40%; (4) the TRS cannot increase the road network capacity within a specific period; however, it can dynamically reduce travel costs and alleviate traffic congestion by improving the network resource supply and demand matching efficiency; and (5) the driver default behavior can increase the V/C ratios and travel costs of all roads in the network.

The results and conclusions have theoretical and practical significance for the implementation of TRS on urban roads. Theoretically, it is proven that the reservation transportation mode is beneficial for promoting the time-space balance between supply and demand to alleviate traffic congestion and realise the transition from user to system optimal transition. Practically, the proposed ORV and reservation tendency ratio can help managers and decision makers determine the critical parameters for implementing the TRS.

This study utilised the SFI to estimate the ORV for urban roads, but the dynamic nature of road capacity and fluctuating traffic demands may affect the accuracy of this estimation. Furthermore, while the TRS shows potential in improving the resource supply-demand match in urban networks, it does not consider shifts in residents' daily travel behavior after implementation. This omission can influence the strategy's efficacy, especially given that driver default behavior has the potential to alter V/C ratios and travel costs across the network. Future research will aim to capture these dynamic behaviors more comprehensively.

Data Availability

The data used to support the findings of this study are available from the corresponding author upon request.

Conflicts of Interest

The authors declare that they have no conflicts of interest.

Authors' Contributions

Ruiyu Zhou was responsible for conceptualization, methodology, data curation, and original draft preparation. Hengrui Chen was responsible for software, investigation, review and editing, project administration, and funding acquisition. Hong Chen was responsible for supervision and methodology.

Acknowledgments

This work was supported by the Fujian University of Technology research start-up project (no. GY-Z23212).

References

[1] Z. Wang, Y. Yang, E. Yao, Y. Zhu, and Z. Rao, "An analysis of commute mode choice behavior considering the impacts of built environment in Beijing," *Transportation Letters*, vol. 14, no. 7, pp. 733–739, 2022.

[2] Z. Liu, H. Chen, Y. Li, and Q. Zhang, "Taxi demand prediction based on a combination forecasting model in hotspots," *Journal of Advanced Transportation*, vol. 2020, Article ID 1302586, 13 pages, 2020.

[3] W. Liu, H. Yang, and Y. Yin, "Efficiency of a highway use reservation system for morning commute," *Transportation Research Part C: Emerging Technologies*, vol. 56, pp. 293–308, 2015.

[4] H. Akahane and M. Kuwahara, "A basic study on trip reservation systems for recreational trips on motorways," in *Proceedings of the 3rd World congress on Intelligent Transportation Systems*, pp. 1–7, San Francisco, CA, USA, November 1996.

[5] C. Menelaou, P. Kolios, S. Timotheou, C. Panayiotou, and M. Polycarpou, "Controlling road congestion via a low-complexity route reservation approach," *Transportation Research Part C: Emerging Technologies*, vol. 81, pp. 118–136, 2017.

[6] Y. Zhao, K. Triantis, D. Teodorović, and P. Edara, "A travel demand management strategy: the downtown space reservation system," *European Journal of Operational Research*, vol. 205, no. 3, pp. 584–594, 2010.

[7] C. Menelaou, P. Kolios, S. Timotheou, and C. Panayiotou, "Effective multi-region traffic control and demand management using an overlay route-reservation scheme," in *Proceedings of the 2018 21st International Conference on Intelligent Transportation Systems*, pp. 1852–1857, Maui, HI, USA, November 2018.

[8] X. Bai, Z. Zhou, K. Chin, and B. Huang, "Evaluating lane reservation problems by carbon emission approach," *Transportation Research Part D: Transport and Environment*, vol. 53, pp. 178–192, 2017.

[9] S. Zhang, Q. Hui, X. Bai, and R. Sun, "Bilevel optimization for the hazmat transportation problem with lane reservation," *Journal of Advanced Transportation*, vol. 2020, Article ID 2530154, 14 pages, 2020.

[10] C. Menelaou, P. Kolios, S. Timotheou, and C. Panayiotou, "Congestion free vehicle scheduling using a route reservation strategy," in *Proceedings of the 2015 18th International Conference on Intelligent Transportation Systems*, pp. 2103–2108, Gran Canaria, Spain, September 2015.

[11] P. Wang, K. Wada, T. Akamatsu, and T. Nagae, "Trading mechanisms for bottleneck permits with multiple purchase opportunities," *Transportation Research Part C: Emerging Technologies*, vol. 95, pp. 414–430, 2018.

[12] C. Menelaou, S. Timotheou, P. Kolios, and C. Panayiotou, "Flexible route-reservations through pricing," in *Proceedings of the 2020 23rd International Conference on Intelligent Transportation Systems*, pp. 1–6, Rhodes, Greece, September 2020.

[13] K. Liu, S. Son, V. Lee, and K. Kapitanova, "A token-based admission control and request scheduling in lane reservation systems," in *Proceedings of the 14th International IEEE Conference on Intelligent Transportation Systems (ITSC)*, pp. 1489–1494, Washington, DC, USA, October 2011.

[14] D. Chandramohan, A. Dumka, V. Dhilipkumar, and J. Loganathan, "Data dissemination for green-VANETs communication: an opportunistic optimization approach," *International Journal of Pervasive Computing and Communications*, vol. 17, no. 1, pp. 89–108, 2021.

[15] C. Menelaou, S. Timotheou, P. Kolios, and C. Panayiotou, "Estimating the critical density of road transportation networks using infinitesimal perturbation analysis of hybrid systems," in *Proceedings of the 2018 Conference on Decision*

and Control, pp. 1809–1814, Miami Beach, FL, USA, December 2018.

[16] J. Geistefeldt and S. Shojaat, “Comparison of stochastic estimates of capacity and critical density for U.S. And German freeways,” *Transportation Research Record: Journal of the Transportation Research Board*, vol. 2673, no. 8, pp. 388–396, 2019.

[17] J. Dong and H. Mahmassani, “Flow breakdown, travel reliability and real-time information in route choice behavior,” *Transportation and Traffic Theory 2009: Golden Jubilee*, pp. 675–695, Springer, Berlin, Germany, 2009.

[18] W. Brilon, J. Geistefeldt, and M. Regler, “Reliability of freeway traffic flow: a stochastic concept of capacity,” in *Proceedings of the 16th International Symposium on Transportation and Traffic Theory*, pp. 125–144, Jerusalem, Israel, July 2005.

[19] S. Shojaat, J. Geistefeldt, S. Parr, C. Wilmot, and B. Wolshon, “Sustained flow index: stochastic measure of freeway performance,” *Transportation Research Record: Journal of the Transportation Research Board*, vol. 2554, no. 1, pp. 158–165, 2016.

[20] S. Shojaat, J. Geistefeldt, S. Parr, L. Escobar, and B. Wolshon, “Defining freeway design capacity based on stochastic observations,” *Transportation Research Record: Journal of the Transportation Research Board*, vol. 2672, no. 15, pp. 131–141, 2018.

[21] H. Chen, R. Zhou, H. Chen, and A. Lau, “Static and dynamic resilience assessment for sustainable urban transportation systems: a case study of Xi ’an, China,” *Journal of Cleaner Production*, vol. 368, Article ID 133237, 2022.

[22] H. Chen, R. Zhou, H. Chen, and A. Lau, “A resilience-oriented evaluation and identification of critical thresholds for traffic congestion diffusion,” *Physica A: Statistical Mechanics and its Applications*, vol. 600, Article ID 127592, 2022.

[23] Q. Lu, T. Tettamanti, D. Hörcher, and I. Varga, “The impact of autonomous vehicles on urban traffic network capacity: an experimental analysis by microscopic traffic simulation,” *Transportation Letters*, vol. 12, no. 8, pp. 540–549, 2020.

[24] L. Elefteriadou, A. Kondyli, S. Washburn et al., “Proactive ramp management under the threat of freeway-flow breakdown,” *Procedia- Social and Behavioral Sciences*, vol. 16, pp. 4–14, 2011.

[25] S. Wong and H. Yang, “Reserve capacity of a signal-controlled road network,” *Transportation Research Part B: Methodological*, vol. 31, no. 5, pp. 397–402, 1997.

[26] D. Washington, “Highway capacity manual,” *Special Report*, vol. 1, no. 1, pp. 5–7, 2000.

[27] Z. Liu, H. Chen, E. Liu, and Q. Zhang, “Evaluating the dynamic resilience of the multi-mode public transit network for sustainable transport,” *Journal of Cleaner Production*, vol. 348, Article ID 131350, 2022.

[28] Z. Liu, H. Chen, E. Liu, and W. Hu, “Exploring the resilience assessment framework of urban road network for sustainable cities,” *Physica A: Statistical Mechanics and its Applications*, vol. 586, Article ID 126465, 2022.

[29] Q. Cheng, S. Wang, Z. Liu, and Y. Yuan, “Surrogate-based simulation optimization approach for day-to-day dynamics model calibration with real data,” *Transportation Research Part C: Emerging Technologies*, vol. 105, pp. 422–438, 2019.

[30] A. U. Z. Patwary, W. Huang, and H. Lo, “A link-to-link segment based metamodel for dynamic network loading,” *Transportation Research Part C: Emerging Technologies*, vol. 130, Article ID 103286, 2021.

[31] A. Forrester, A. Sobester, and A. Keane, *Engineering Design via Surrogate Modelling: A Practical Guide*, John Wiley and Sons, Hoboken, NJ, USA, 2008.

[32] D. Bertsekas and E. Gafni, “Projection method for variational inequalities with applications to the traffic assignment problem,” *Mathematical Programming Studies*, vol. 17, pp. 139–159, 1987.

[33] A. Chen, D. Lee, and R. Jayakrishnan, “Computational study of state-of-the-art path-based traffic assignment algorithms,” *Mathematics and Computers in Simulation*, vol. 59, no. 6, pp. 509–518, 2002.

[34] D. Lee, Y. Nie, and A. Chen, “A conjugate gradient projection algorithm for the traffic assignment problem,” *Mathematical and Computer Modelling*, vol. 37, no. 7-8, pp. 863–878, 2003.

[35] D. Jones, M. Schonlau, and W. Welch, “Efficient global optimization of expensive black-box functions,” *Journal of Global Optimization*, vol. 13, no. 4, pp. 455–492, 1998.

[36] Z. Han, “Kriging surrogate model and its application to design optimization: a review of recent progress,” *Acta Aeronautica et Astronautica Sinica*, vol. 37, pp. 3197–3225, 2016.

[37] M. Patkar and A. Dhamaniya, “Effect of on-street parking on effective carriageway width and capacity of urban arterial roads in India,” *European Transport-trasporti Europei*, vol. 73, 2019.